ULTRATHIN MANGANITE LAYERS

O. Shapoval

Institute of Electronic Engineering and Nanotechnologies, Academy of Science of Moldova, Academiei str. 3/3, Chisinau, MD 2028 Republic of Moldova
e-mail: shapoval@nano.asm.md

(Received 4 October 2011)

Abstract

Epitaxial La-deficient ultrathin films of $La_{1-\delta}MnO_3$ (LMO) were grown by a metalorganic aerosol deposition technique with monolayer accuracy on $SrTiO_3$ (STO) substrates and engineered by using different interfacial layers. The role of LaO-TiO_2 interface in the formation of the ferromagnetic metallic state in very thin LMO films was demonstrated. The ferromagnetic metallic ground state in LMO films with the thickness down to 6 monolayers is stabilized by a combination of a La-deficiency and the interface-induced doping.

1. Introduction

To enhance the functionality of all-oxide based devices, the idea of the interface engineering of multilayered oxide heterostructures was put forward in the last few years. $LaMnO_3$ (LMO) is one of the promising materials used for the interfacial design of different multilayer systems. The stoichiometric LMO with the nominal $t^3_{2g}e^1_g$ occupancy of Mn^{3+} ions is an insulator with strong Mott-Hubbard correlations in a half-filled e_g band [1]. An *A*-type antiferromagnetic (AFM) ground state originates due to the orbital ordering of e_g-orbitals with ferromagnetic (FM) in-plane and AFM out-of-plane exchange interactions. Nevertheless, LMO can be easily transformed into an FM metal, particularly in thin films [2] and superlattices of LMO/SMO [3] and LMO/STO [4]. The ferromagnetism was shown to be due to the change of: (a) stoichiometric cationic composition; (b) optimal oxygen content as well as (c) due to epitaxial stabilization of a nonstoichiometric state in the layers grown on the $SrTiO_3$ (STO) (100) substrates [2, 5]. The "electron leakage" phenomenon, which is caused by the polar discontinuity at the interfaces, was shown to control the magnetotransport in superlattices [4, 6]. The main parameter that affects the direction of charge leakage and, therefore, the magnetic properties is the substrate-induced epitaxial strain. The interest in LMO as a functional material has been recently stirred up by the demonstration of a metal-insulator transition at T_{MI} >400 K in heavy La-deficient films [7].

An important question concerning electronic and structural reconstruction at the interfaces is the atomic structure of stacking planes. The LMO/SMO system demonstrates exclusively the LaO-MnO_2-SrO sequence of atomic planes at the interface [8]. In contrast, the LMO/STO system reveals two types of interfaces due to different A- and B-site occupancies in the perovskite lattices. Namely, (1) (LaO-MnO_2)-(SrO-TiO_2) (compactly MnO_2-SrO) and (2) (MnO_2-LaO)-(TiO_2-SrO) (or LaO-TiO_2) [9] interfaces were observed. In this case, one should expect different interface-induced properties [10]. An example of these different properties attributed to A^1O-B^2O_2 and A^2O-B^1O_2 interfaces for the $A^1B^1O_3$-$A^2B^2O_3$ stacked perovskites was demonstrated for the well-known $LaAlO_3/SrTiO_3$ system [11], where AlO_2-LaO-TiO_2 stacked

planes are electronically reconstructed and exhibit a metallic behavior, whereas the AlO_2-SrO-TiO_2 interface is insulating due to atomic reconstruction.

A single heterojunction for an $A^1B^1O_3$ layer grown on the STO(100) substrate, can be modified by TiO_2- or SrO-termination of the substrate surface. In the case of multilayered $A^1B^1O_3$-$A^2B^2O_3$ structures a conventional growth techniques produce two types of interfaces [9]. The first layer starts from A^1O-plane on TiO_2-terminated surface STO(100) substrate and terminates by B^1O_2-plane; the next layer repeats the alternation of AO- and BO_2-planes. A possibility to tailor the superlattices with single type of interface by introducing an extra-plane was recently demonstrated for the LMO/STO system [4]. The presence of extra LaO-planes in manganite layers and TiO_2-planes in titanate layers was confirmed by STEM combined with electron-energy-loss spectroscopy (EELS) analysis.

The aim of the presented work was to study the magnetotransport properties of ultrathin LMO films with the thicknesses comparable to the thickness of single layers in SLs. To design the LMO-based layered structures with optimized FM metallic behavior two approaches were applied: (1) the La-deficiency was intentionally generated in the LMO layer and (2) ultrathin LMO films were engineered by different interfaces.

2. Experimental

The samples were prepared by a metalorganic aerosol deposition (MAD) technique, elaborated earlier for the preparation of complex oxide thin films and further developed for the deposition of ultrathin films and superlattices [12]. Aerosols of organic solutions, which contained metal β- diketonates (e.g. La-, Sr-, Mn-acetylacetonates), were sprayed onto a heated substrate. A film grows on the substrate as a result of a heterogeneous pyrolysis reaction of the metalorganic component. Within the MAD technique, one can easily manipulate the precursor solutions, which contain either a single precursor for mono-oxide layers or a mixture of two and more precursors to produce layers of complex oxides. The monolayer accuracy was achieved by accurate calibration of dosing units. Vacuum-free MAD technique allowed us to interrupt deposition process and to continue the preparation of the layered structure after intermediate express measurements.

The STO(100) substrate was chosen due to the possibility to study the influence of both surface terminations. The atomically smooth TiO_2-terminated STO(100) with terrace steps of one unit cell in height was obtained by treating the crystal surface with a pH-controlled NH_4F-HF solution [13]. The AFM image of the TiO_2-terminated STO(100) surface is shown in Fig.1a.

The SrO-terminated surface was produced by deposition of a SrO monolaeyer (ML) on the TiO_2- terminated surface. The exact oxygen stoichiometry in the prepared $LaMnO_3$ layers was assumed due to high (atmospheric) gas pressure conditions [12]. As the criteria of a stoichiometric La/Mn=1:1 relation, we used the insulating behavior of the film, which is unique for a stoichiometric LMO, as well as smooth and flat surface morphology (Fig. 1b) with terraces inherited from STO. The deviation of the La molar content from the “right” La/Mn-ratio in the solution was used in the sequel as a measure of the La-deficiency. The La-deficiency of LMO layers was varied in a range of 0-12%. The thickness of LMO films was d = 6-30 unit cells (u.c.) or d = 2.5-12 nm.

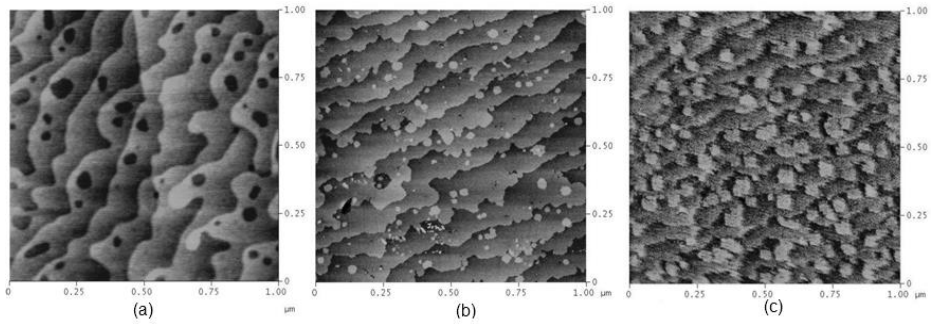


Fig. 1. Scanning probe topographic images of: (a) the TiO_2-terminated STO(100) substrate (AFM), (b) 10-nm LMO layer deposited on the TiO_2-terminated surface of the STO(100) substrate (STM), (c) the STO cap layer on the LMO/STO(100) structure (STM).

LMO layers were deposited directly onto both TiO_2- and SrO-terminated substrates or onto the STO surface, buffered by 2 u.c. of SMO. The top surface of LMO films remained free or covered by 2 u.c. of the cap layer, e.g., STO (Fig. 1c) or SMO.

The elemental maps were obtained by high resolution EELS data using background subtraction and peak integration and applied to investigate the interface structure. Electron transport measurements were performed by a standard 4-probe technique using a commercial PPMS from "Quantum Design". Magnetization was measured by means of a commercial SQUID (MPMS, "Quantum Design").

3. Results and discussion

The growth of LMO on the TiO_2-terminated STO(100) from a solution containing both La and Mn precursors occurs in the following way. It starts from LaO-plane, forming the LaO-TiO_2 interface (Fig. 2). The maps indicate a (TiO_2) atomic-plane termination for the STO substrate and the LMO layer starts with the (LaO) plane.

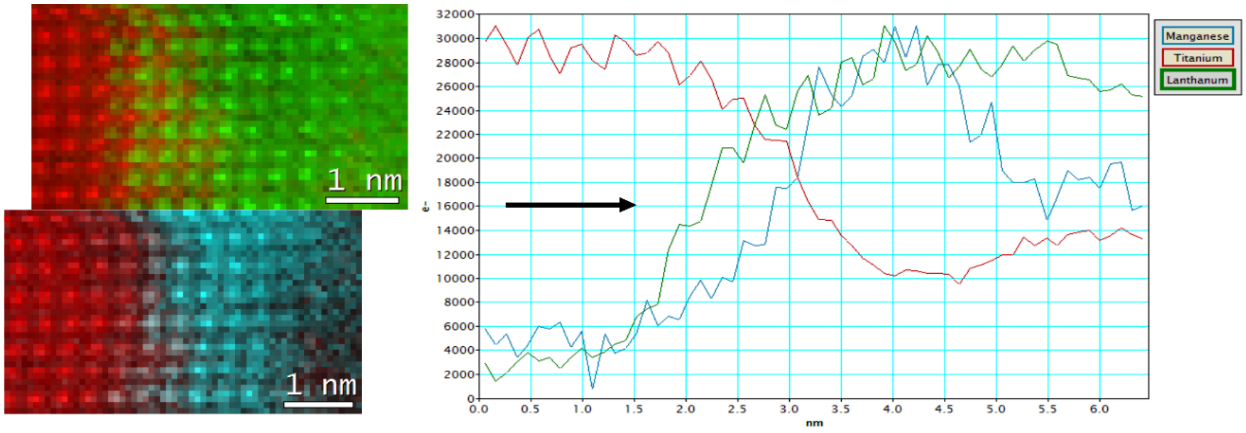


Fig. 2. Color maps of La/Ti (top) and Mn/Ti (bottom) (Ti=red; La=green; Mn=blue) and EELS signal profiles of LMO-STO interface.

The role of the LaO-TiO_2 interface was examined using a set of samples with the same La-deficiency, δ=6 %, and thickness of the LMO layer. The influence of LaO-TiO_2 interfaces on the electron transport as a function of temperature is shown in Fig. 3. Thus, the LMO film with

one (bottom) LaO-TiO_2 interface and free surface (top) was prepared after deposition of 26 perovskite unit cells of LMO. This film demonstrates a metal-insulator (MI) transition at T_{MI}=285K and a metallic behavior at low temperatures (curve *1*, Fig. 3). The deposition of one monolayer of LaO followed by 2 u.c. of STO on the top surface of the LMO film resulted in the enhancement of T_{MI} by 45 K and in the decrease of the resistance at T_{MI} by 2 times (curve *2*, Fig. 3). An LMO film without LaO-TiO_2 interfaces was prepared by the deposition of one monolayer of SrO onto the TiO_2-terminated STO(100) prior to the deposition of LMO. In this case, the manganite had to start the growth from the MnO_2 plane. The LMO film with the bottom SrO-MnO_2 interface and free top surface shows a decreased T_{MI}=210K and an insulating behavior at low temperatures (curve *3*, Fig. 3). The deposition of 2 u.c. of STO on the top of the LaO-terminated manganite film results in the formation of an LaO-TiO_2 top interface, thus, recovering the transport (curve *4*, Fig. 3) to that described above for the film with one LaO-TiO_2 bottom interface.

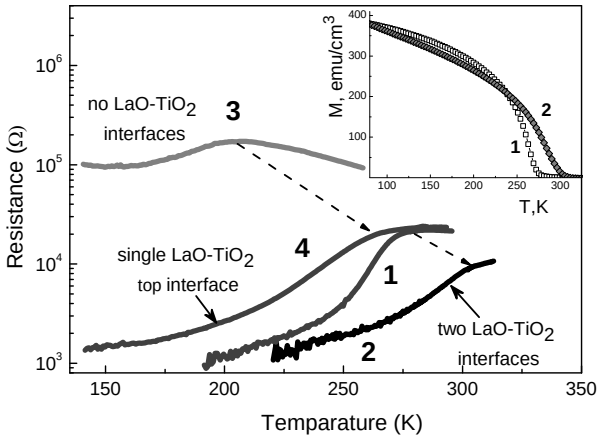


Fig. 3. Evolution of the transport properties of 10 nm LMO layers deposited on the STO(100) substrates and equipped with: (*1*) bottom LaO-TiO_2 interface; (*2*) top and bottom LaO-TiO_2 interfaces; (*3*) no LaO-TiO_2 interface; (*4*) top LaO-TiO_2 interface. Insert: Magnetization as a function of temperature.

The metallic behavior in LMO engineered films is optimized because each LaO-TiO_2 interface creates effective conductive channels close to (or inside) the LMO layer. Magnetization as a function of temperature (see inset to Fig. 3) reveals, however, an unexpected behavior: after adding the second LaO-TiO_2 interface, the Curie temperature (T_C) was increased up to 305 K (the film with one interface shows T_C=275 K). The increase of T_C correlates with the increase of T_{MI}, but T_C is consistently lower than T_{MI}. Surprisingly, the saturation magnetization and magnetic hysteresis did not change after adding the second interface, M_S~400 emu/cm^3~2.5 μ_B/Mn. This value is larger than that for undoped LMO [14] but it is significantly lower than magnetization for optimal doped manganites, M_S~3.7 μ_B/Mn [15]. The relatively high residual resistivity, $\rho_{10K}=1.6\cdot10^{-4}$ Ωcm, also indicates insufficient doping level.

The magnetic and transport properties of the samples with different thickness and the same La deficiency of LMO layers (see Fig. 4) stay in line with the probably lowered doping level. The highest temperature of the metal-insulator transition $T_{MI}\approx$330 K was achieved in LMO with the thickness of 26 u.c. and La-deficiency, δ=6-8 %. The resistance exhibits a metallic behavior down to the lowest temperature. With decreasing thicknesses of the LMO layer, a decrease of T_{MI}

and an increase of the resistance were observed. The thickness dependence of the transport properties can be rationalized within the "electron leakage" from the interface into the LMO layer. The reduced oxidation state in the sample is consistent with some degree of electron doping coming from the electron from the extra (LaO) plane. The depth of charge spreading is larger than 2 u.c. as calculated for the insulating LMO [6]; it looks like charge is evenly distributed among the tens of LMO unit cells [4]. By reducing the thickness of LMO, one extra-electron distributed among smaller amount of LMO unit cells would give a stronger reduction of the averaged oxidation state. This scenario suggests that LMO layers become progressively less hole-doped as the thickness is reduced; that is, it is consistent with an increased electron leakage into LMO. Finally, for samples thinner than 3 nm (6-7 uc) no metallic behavior was observed any longer regardless of the La deficiency; note that the 2.5-nm-thick film still remains ferromagnetic.

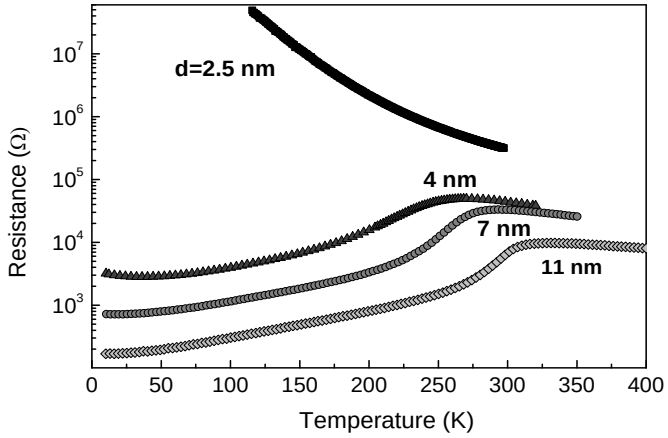


Fig. 4. Temperature dependence of the transport properties of the STO-LMO-STO structures with different LMO layer thickness.

A further support for the above model comes from magnetization measurements. We observed a gradual decrease of MS with decreasing of the LMO thickness (see Fig. 5a), which correlates with the decrease in both TC and TMI. Magnetic hysteresis behavior also comes to agreement with this model. The value of coercive field H_C ~30 Oe indicates magnetic homogeneity of the 26-u.c.-thick film. Apparently (see Fig. 5b), magnetic inhomogeneity increases and the saturation magnetization decreases dramatically with decreasing thickness, i.e., M_S<1 μ_B/Mn for the 6-uc-thick film, which is typical for an undoped LMO [14]. From a magnetic point of view only, the system looks like a weak ferromagnet. However, the e_g-hole is localized within certain regions with very few Mn-ions. The ground state is a mixed state composed of disordered nanosized "double-exchange" metallic clusters and coexisting insulating domains. Even for high magnetic fields the system with magnetically aligned FM clusters does not reach the percolation limit [16] even if they grow in size.

Inversion of the LaO-TiO_2 interface to SrO-MnO_2 by introducing SrO extra-layer (see Fig. 3) leads to the degradation of transport properties. A new design of SrO-MnO_2 could improve the magnetotransport in LMO layer. According to the calculations [6], the Mn e_g electrons leak out from the LMO layer to the SMO one and change the magnetism at the interface, while away from the interface, the magnetism of the respective bulk materials is preserved. Introduction of the 2 u.c. of SMO as buffer and cape layers allowed us to change the direction of the charge leakage and as a consequence, to restore the metallic behavior in very thin LMO films.

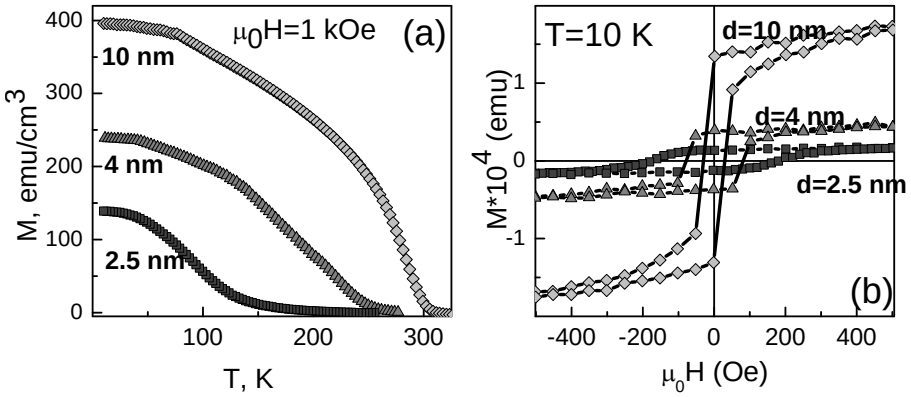


Fig. 5. Magnetization as a function of temperature (a) and magnetic histeresis (b) for the STO-LMO-STO structures with different thickness of LMO layers.

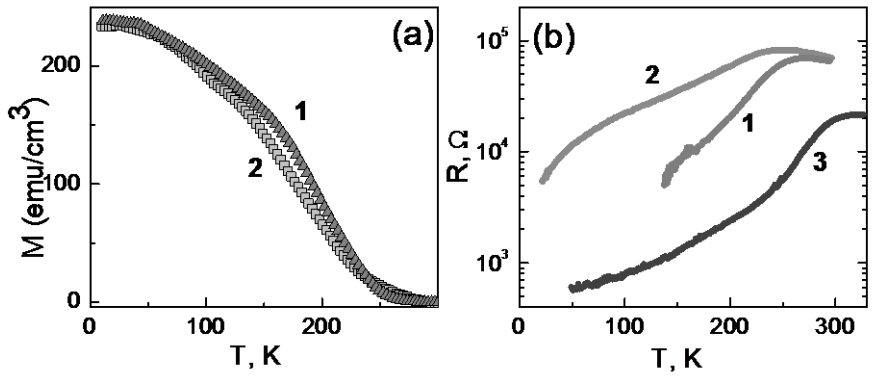


Fig. 6. Magnetization as a function of temperature (a) and resistance as function of temperature (b) for (*1*) the STO-LMO(10 ML)-STO, (*2*) SMO-LMO(6 ML)-SMO, and (*3*) SMO-LMO(10 ML)-SMO structures.

The resistance of the SMO-LMO-SMO structure was found to be about 5 times lower than the resistance for the STO-LMO-STO sample with the same thickness (10 u.c.) and La-deficiency (see Fig. 6b). The LMO film confined by 2 SMO u.c. demonstrates metallic behavior down to the thickness of 6 u.c. The saturation magnetization and T_C of SMO-LMO(6 u.c.)-SMO and STO-LMO(10 u.c.)-STO are very similar (Fig. 5a), but the thinning of LMO layer, in any way, leads to an increase in inhomogeneity, which is shown in the increased resistance (curve *2* in Fig. 6b). It is worth noting that the upper limit of the layer thickness is absent in the case of the La-deficient LMO with a ferromagnetic metallic behavior.

3. Conclusion

The tailoring of the interfaces can be very effective in modifying the magnetotransport properties of ultrathin LMO films. The combination of the doping effects due to the La-deficiency with the interface-induced doping allowed us to preserve the ferromagnetic metallic behavior in the STO-LMO-STO structures with the thickness down to 10 u.c. of LMO. Interface modification of LMO layers by the 2-u.c.-thick SMO bottom and top interfaces led to a further shrinkage of the metallic LMO layer thickness down to 6 u.c. The engineering of the single type LaO-TiO_2 interface in the STO/LMO stacked perovskites can be performed within the

MAD technique by deposition of an extra LaO plane. Thus, we show the possibility to change the natural growth sequence, i.e., AO-BO_2, along the <100> direction of the perovskite structure.

Acknowledgements

The author thanks V. Moshnyaga and A. Belenchuk for maintenance of this investigation. The data of HRTEM analysis performed by S. Lichtert EMAT, University of Antwerp is highly appreciated.

References

[1]A. Yamasaki, M. Feldbacher, Y. F. Yang, O. K. Andersen, and K. Held, Physical Review Letters 96, 166401 (2006).
[2]A. Gupta, T. R. McGuire, P. R. Duncombe, M. Rupp, J. Z. Sun, W. J. Gallagher, and Gang Xiao, Applied Physics Letters 67, 3494 (1995).
[3]A. Bhattacharya, S. J. May, S. G. E. te Velthuis, M. Warusawithana, X. Zhai, Bin Jiang, J. M. Zuo, M. R. Fitzsimmons, S. D. Bader, and J. N. Eckstein, Physical Review Letters 100, 257203 (2008).
[4]J. Garcia-Barriocanal, F. Y. Bruno, A. Rivera-Calzada, Z. Sefrioui, N. M. Nemes, M. Garcia-Hernández, J. Rubio-Zuazo, G. R. Castro, M. Varela, S. J. Pennycook, C. Leon, and J. Santamaria, Advanced Materials 22, 627 (2010).
[5]P. Orgiani, C. Aruta, R. Ciancio, A. Galdi, and L. Maritato, Applied Physics Letters 95, 013510 (2009).
[6]B. R. K. Nanda and S. Satpathy, Physical Review B 81, 224408 (2010).
[7]P. Orgiani, A. Galdi, C. Aruta, V. Cataudella, G. De Filippis, C. A. Perroni, V. Marigliano Ramaglia, R. Ciancio, N. B. Brookes, M. Moretti Sala, G. Ghiringhelli, and L. Maritato, Physical Review B 82, 205122 (2010).
[8]J. Verbeeck, O. I. Lebedev, G. Van Tendeloo, and B. Mercey, Physical Review B 66, 184426 (2002).
[9]M. Varela, H. M. Christen, H. N. Lee, L. Petit, T. Schulthess, S. J. Pennycook, W. Luo, S. T. Pantelides, J. Garcia-Barriocanal, C. Leon, and J. Santamaria, Microscopy and Microanalysis 14, 1346 (2008).
[10] H. Zenia, G. A. Gehring, G. Banach, and W. M. Temmerman, Physical Review B 71, 024416 (2005).
[11] D. H. A. Blank J. Mannhart, H. Y. Hwang, A. J. Millis, and J.-M. Triscone, MRS Bulletin 33, 1027 (2008).
[12] K. Gehrke, V. Moshnyaga, K. Samwer, O. I. Lebedev, J. Verbeeck, D. Kirilenko, and G. Van Tendeloo, Physical Review B 82, 113101 (2010).
[13] M. Kawasaki, K. Takahashi, T. Maeda, R. Tsuchiya, M. Shinohara, O. Ishiyama, T. Yonezawa, M. Yoshimoto, and H. Koinuma, Science 266, 1540 (1994).
[14] C. Adamo, X. Ke, P. Schiffer, A. Soukiassian, M. Warusawithana, L. Maritato, and D. G. Schlom, Applied Physics Letters 92, 112508 (2008).
[15] J. M. D. Coey, M. Viret, and S. von Molnár, Advances in Physics 48 (2), 167 (1999).
[16] P. A. Algarabel, J. M. De Teresa, J. Blasco, M. R. Ibarra, Cz. Kapusta, M. Sikora, D. Zajac, P. C. Riedi, and C. Ritter, Physical Review B 67, 134402 (2003).